HHS Public Access

Author manuscript

FASEB J. Author manuscript; available in PMC 2022 March 10.

Published in final edited form as:

FASEB J. 2020 September ; 34(9): 11685–11697. doi:10.1096/fj.202000888R.

Erythropoietin signaling in osteoblasts is required for normal bone formation and for bone loss during erythropoietin stimulated erythropoiesis

Sukanya Suresh[*], **Jeeyoung Lee**, **Constance Tom Noguchi**

Molecular Medicine Branch, National Institute of Diabetes and Digestive and Kidney Diseases, National Institutes of Health, Bethesda, MD 20892 USA.

Abstract

Erythropoietin (EPO) regulates erythropoiesis by binding to erythropoietin receptor (Epor) on erythroid progenitor cells. Epor is also expressed on bone forming osteoblasts and bone loss accompanies EPO stimulated erythropoiesis in mice. Mice with Epor restricted to erythroid tissue exhibit reduced bone and increased marrow adipocytes; in contrast, transgenic mice (Tg) with osteoblastic-specific deletion of *Epor* exhibit reduced trabecular bone with age without change in marrow adipocytes. By 12 weeks, male Tg mice had 22.2% and female Tg mice had 29.6% reduced trabecular bone volume compared to controls. EPO administration (1200 U/kg) for ten days reduced trabecular bone in control mice but not in Tg mice. There were no differences in numbers of osteoblasts, osteoclasts and marrow adipocytes in Tg mice, suggesting independence of EPO signaling in mature osteoblasts and adipocytes. Female Tg mice had increased number of dying osteocytes and male Tg mice had a trend for more empty lacunae. Osteogenic cultures from Tg mice had reduced differentiation and mineralization with reduced *Alpl* and *Runx2* transcripts. In conclusion, endogenous EPO-Epor signaling in osteoblasts is important in bone remodeling, particularly trabecular bone and endogenous Epor expression in osteoblasts is required for bone loss accompanying EPO stimulated erythropoiesis.

Keywords

EPO; bone remodeling; trabecular; osteoblast differentiation; osteocyte

Introduction

Erythropoietin (EPO), a hematopoietic cytokine secreted by the fetal liver and adult kidneys is essential for erythropoiesis. Binding of EPO to EPO receptor (Epor) expressed on erythroid progenitor cells stimulates their survival, proliferation and differentiation to red

Corresponding author: Constance Tom Noguchi; Molecular Medicine Branch; National Institute of Diabetes and Digestive and Kidney Diseases; National Institutes of Health; Building 10, Room 9N319; 10 Center Drive, MSC-1822; Bethesda, MD 20892-1822 USA; connien@niddk.nih.gov; Tel.: +1-301-496-1163; Fax: +1-301-402-0101.

[*]Present address: Endocrinology, R3, C110 ENDC, Indiana University, Indianapolis, IN

Author contributions

SS designed and performed experiments, collected and analyzed the data, wrote the manuscript. JL collected the data and edited the manuscript. CTN developed the concept, supervised the study and wrote the manuscript.

blood cells. Clinically, recombinant human EPO is used to treat anemia in chronic kidney disease and anemia associated with cancer chemotherapy(1). Functional Epor is expressed in several non-erythroid cells including adipocytes(2), endothelial cells(3), osteoclasts(4), osteoblasts, bone marrow stromal cells, astrocytes(5) and myoblasts(6), suggesting a systemic effect for EPO beyond its principal role in erythropoiesis.

Bone is a dynamic organ that undergoes continuous remodeling due the coupled activity of osteoclasts and osteoblasts. Osteoclasts remove the mineralized bone resulting in resorptive pits which are then filled by extracellular matrix synthesized by osteoblasts leading to bone formation. Constant bone remodeling replaces old bone with new bone and repairs any damages in bone architecture. The proper regulation of osteoclast and osteoblast activity is essential for controlled bone development(7).

In bone, elevated EPO signaling has distinct effects. In fracture models, EPO administration promotes bone formation and repair(8, 9). In contrast, elevated EPO production in transgenic mice as well as exogenous EPO administration in healthy C57BL6 mice resulted in bone reduction associated with increased osteoclast activity(4). Previous studies have also reported EPO production in osteoblasts and an increase in osteoblasts in mice treated with EPO(10). However, the role of endogenous EPO signaling specifically in osteoblasts in bone development and maintenance is not known.

In this study, to determine the direct contribution of EPO signaling in osteoblasts to bone formation, we generated a transgenic mouse model (Tg) where *Epor* is deleted specifically in osteoblasts. We observed that *Epor* deletion in osteoblasts impaired their differentiation *in vitro* and reduced trabecular bone in both male and female mice. These findings demonstrate that endogenous EPO signaling directly regulates osteoblasts thus providing a novel role for EPO as an essential regulator of bone homeostasis. Furthermore, in contrast to bone reduction with EPO treatment in wild type (wt) mice, bone reduction was not observed in Tg mice with exogenous EPO administration, suggesting that bone loss with EPO treatment is a direct consequence of osteoblast response to EPO mediated via osteoblast Epor activation.

Materials and Methods

Animal studies

Transgenic mice with osteoblast specific deletion of *Epor* (Tg) were generated by crossing *Osteocalcin (Bglap)-Cre* mice (Jackson laboratories, ME, US) with $Epor^{floxp/floxp}$ mice in a C57BL/6 background as described previously(11). The resulting pups of first generation carrying both the *Cre* and *loxp* sequences were then used as breeding pairs to generate mice with homozygous deletion of *Epor* in osteoblasts. Mice expressing only *Cre* were used as littermate controls (wt). Presence of the transgene was confirmed using the following primers, *Osteocalcin-Cre*: Forward primer 5'-CAA ATA GCC CTG GCA GAT TC-3', reverse primer 5'-TGA TAC AAG GGA CAT CTT CC-3'; *loxp*: Forward primer 5'- CTC CTG GAG CAC CTA TGA CC-3', reverse primer- CCCGTTCTTGGCTCAAAGCCAATC. Ten-week-old male and female Tg mice and their littermates were administered either saline or EPO (Epogen, Amgen, Thousand Oaks, CA) at 1200 U/kg daily for ten days. Fat mass and lean mass measurements were performed before the beginning of EPO administration

and after the study duration using the EchoMRI 3-in-1 device (Echo Medical Systems, Houston, TX, USA). Hematocrits were measured after the last day of EPO treatment as previously described(12).

Micro-CT

Mouse femurs were analyzed using a Bruker Skyscan 1172 micro-CT scanner ((Micro Photonics Inc, PA, USA). Trabecular and cortical bone were analyzed at 0.35 mm and 4.25 mm from the growth plate respectively. For both regions, 1.5 mm of femurs sections comprising 257 bone slices were individually analyzed using CTAn software at 6 μm resolution and 3D models of regions of interest were constructed.

Histology, H & E and TRAP staining

Mouse femurs were fixed in 10% buffered neutral formalin (Sigma, MO, USA) for 24h followed by decalcification in 10% ethylenediaminetetraacetic acid (0.5 M) at 4°C until complete decalcification was confirmed by x-ray analysis. Hematoxylin-Eosin (H&E) staining was performed on 6 μm sections of decalcified paraffin embedded femurs to assess bone and bone marrow histology. For marrow adiposity, the number of adipocytes were expressed in terms of marrow area. Osteoblasts lining the trabecular bone were identified from the H & E stained femur sections, number of cells were expressed in terms of the bone surface. H & E stained sections were also used for enumerating alive, dying and dead osteocytes in the cortical bones using a previously published method(13). For osteoclast detection in femurs, Tartrate-resistant acid phosphatase (TRAP) staining was performed using TRAP/ALP Stain Kit according to manufacturer's instructions (# 294-67001, Wako Chemicals, USA). For all measurements, a minimum of three separate fields were analyzed from each bone section. All measurements were performed using ImageJ software.

Osteogenic cultures

Calvarial osteogenic cells were isolated from 6–8-week-old mice using previously described protocol. Proliferation of osteogenic cells was measured using Thiazolyl Blue Tetrazolium Blue (MTT) assay (Sigma). Alkaline phosphatase (ALP) activity was quantified using SIGMAFAST™ p-Nitrophenyl phosphate Tablets (Sigma). For microscopic observation of ALP activity, SIGMA FAST™ BCIP/NBT (5-Bromo-4-chloro-3-indolyl phosphate/Nitro blue tetrazolium) tablets were used according to manufacturer's instructions. Mineralization was detected using 1% alizarin staining (pH 4.6). All reagents for measuring ALP activity, ALP visualization and mineralization were purchased from Sigma, MO, USA.

Osteoclast generation from bone marrow

Bone marrow cells were harvested from 8–10-week-old mice and seeded into tissue culture treated plates and allowed to attach overnight in α-MEM medium with 10% fetal bovine serum. Non-adherent cells (5×10^5 cells/cm^2) were plated into 96 flat-bottomed well plates in fresh medium containing 30 ng/mL RANKL and 20 ng/mL M-CSF (Peprotech, NJ, USA). Medium was replaced every other day until osteoclasts appeared (4–5 days). TRAP staining was performed according to manufacturer's instructions (#387-1A, Sigma, St Louis, MO, USA) to visualize osteoclasts.

Bone resorption assays

Non-adherent bone marrow cells (5×10^5 cells/cm^2) harvested from either Tg or wt mice were plated in Corning Osteo Assay Surface 96-well plates (Sigma, St Louis, MO, USA) in α-MEM medium with 10% fetal bovine serum. After overnight incubation, fresh medium containing 30 ng/mL RANKL and 20 ng/mL M-CSF (Peprotech, NJ, USA) was added. Medium was replaced every other day. Once osteoclasts appeared after 4–5 days, cells were washed with 10% bleach solution and plates were air dried. Images of resorption pits on the plates were captured using an EVOS microscope and area of resorption was quantified using ImageJ software.

RNA extraction and real-time PCR

Total RNA was extracted from primary osteogenic cells from calvaria using RNeasy Mini kit (Qiagen, MD, USA) and treated with DNase I (Promega, WI, USA); 1–2 μg was reverse transcribed using MultiScribe Reverse Transcriptase (ABI)) (Thermo Fisher Scientific, MA, USA) for quantitative PCR assays. For mouse *Epor* analysis, Taqman primers and probe and mouse *S16* primers and probe (house-keeping gene) were used as described previously(2). For all other PCR assays, SYBR green real time PCR was carried out using gene specific primers (Table 1) with normalization to house-keeping gene *β-actin* using SYBR Green dye and qPCR SuperMix (Roche Applied Science, IN, USA); relative mRNA quantification was calculated by delta-delta Ct method.

Statistical analysis

Data are expressed as mean ± standard error. Two-tailed non-paired Student's t test was used to determine statistical significance between control and test groups. Comparisons among multiple groups were evaluated using one-way analysis of variance (ANOVA) with Dunnet's multiple comparison post hoc tests at $\alpha=0.05$ (Graphpad Prism 6).

Results

Mice with *Epor* deletion in osteoblasts have reduced bone mass

We used transgenic mouse with *Epor* deletion in osteoblasts (Tg) to assess the role of endogenous EPO signaling in osteoblasts. Tg mice were generated by mating *Epor* floxed mice with mice containing a cre-recombinase controlled by the *Bglap* promoter (*Osteocalcin*) to generate an osteoblast specific knockout of *Epor*. Genotyping showed resulting transgenic mice (Tg) having Cre expression (280 bp) and floxed Epor (490 bp) (Supplemental Figure 1A). Littermates with Cre expression and wild type Epor (450 bp) were used as controls (referred as wt in the text). Primary osteogenic cells isolated from Tg mice showed reduced *Epor* mRNA levels compared to littermate controls (Supplemental Figure 1B). Targeted deletion of *Epor* in osteoblasts did not affect tissues with high *Epor* expression such as spleen, an erythroid organ in mice, and white adipose tissue (WAT) (Supplemental Figure 1C).

In young male Tg mice of 4 weeks of age, micro-CT analysis of femurs showed 11.5% reduction in trabecular bone volume, 13.8% reduction trabecular number and 28.3% reduction in trabecular connectivity density (Figure 1B, 1C, 1F) with no significant effects

in trabecular bone mineral density (BMD), spacing and thickness (Figure 1A, 1D, 1E). Compared with littermate controls, cortical bone of young Tg male mice did not show any significant differences (Figure 1G–1I). Unlike the male mice, the trabecular bone of young female mice was comparable to their littermate controls (Figure 1J–1O). Young female Tg mice had reduced cortical bone thickness (Figure 1R), but their cortical BMD and cortical bone volume were similar to control mice (Figure 1P, 1Q).

By 12 weeks of age, both adult male and female Tg mice exhibited significant reduction in trabecular bone (Figure 2 and Figure 3). Male Tg mice had 22.2% reduced trabecular bone volume, 18.2% reduction in trabecular number, 18.9% increase in trabecular spacing and 27% reduction in connectivity density compared to littermate controls (Figure 2A–2G). There were no significant differences between the cortical bone of Tg male mice and controls. Female Tg mice 12 weeks of age had 29.6% reduction in trabecular bone volume, 24.4% reduction in trabecular number, 19.3% increase in trabecular spacing and 30% reduction in connectivity density relative to control mice (Figure 3A–3G). Female Tg mice at 12 weeks had reduced cortical bone volume but the cortical BMD and thickness were not affected (Figure 3H–3J).

Epor deletion in osteoblasts protects mice from EPO induced bone reduction

Elevated EPO in mice expressing high transgenic EPO and in wild type mice with EPO treatment results in bone reduction(4, 12, 14). To understand if the EPO induced bone reduction is mediated by osteoblasts expressing Epor, we administered daily doses of EPO at 1200 IU/kg for ten days in both male and female Tg mice and their littermate controls. In both control and Tg mice, EPO treatment raised hematocrits to similar levels (Supplemental figure 2A, 2E). In male control mice, EPO administration resulted in 38.4 % reduction in trabecular bone volume, 32.4% reduction in trabecular number and 30.7% increase in trabecular spacing (Figure 2A–2F, Supplemental Table 1). In female control mice, the effects of EPO administration were slightly greater with 40.1% reduction in trabecular bone volume, 40.9% reduction in trabecular number and 32% increase in trabecular spacing (Figure 3A–3G, Supplemental Table 1). Elevated EPO did not affect cortical bone in male or female control mice (Figures 2H–2J, 3H–3J, Supplemental Table 1). In both male and female Tg mice with *Epor* deletion in osteoblasts, EPO administration for ten continuous days did not induce any significant changes, demonstrating the requirement for *Epor* expression in osteoblasts for bone reduction with EPO administration. However, in male Tg mice with EPO administration there was a trend for reduced trabeculae with 20% reduced trabecular bone volume compared to Tg mice administered with saline. There was no significant difference in body weight, fat mass and in lean mass between control and Tg mice with or without this schedule for EPO treatment (Supplemental figures 2B–2D, 2F–2H).

Epor deletion in osteoblasts does not affect marrow adipocytes

We previously reported increased marrow adiposity in mice with erythroid restricted *Epor* expression(12). To determine if lack of *Epor* expression in osteoblasts has any effect on marrow adiposity, the number of adipocytes in the H & E stained sections of femurs of both male and female Tg mice and their littermate controls were determined. There were no

significant differences in the marrow adiposity between the littermate controls and Tg mice in either gender (Figure 4A–4D). As previously reported, female mice have more marrow adiposity than males and there appears to be a tendency for female Tg mice to have even more marrow adiposity. Elevated EPO reduced marrow adipocytes in all mice receiving EPO.

Epor deletion in osteoblasts reduces their differentiation and mineralization *in vitro*

Primary osteogenic cells isolated from the calvaria of Tg mice cultured in osteogenic medium showed reduced differentiation potential compared to the osteogenic cells from littermate control mice assayed on days 7, 14 and 21 (Figure 5A). With long term osteogenic cultures, the Tg osteogenic cells had less ALP activity on all days of measurement compared to wt osteogenic cells (Figure 5B). The Tg osteogenic cells also had reduced *Alpl* and *Runx2* expression, but did not have any significant change in *Osterix* levels (Figure 5C). Addition of EPO to the osteogenic cultures from Tg mice did not affect their differentiation whereas wt osteogenic cells had decreased differentiation with EPO treatment (Figure 5D). Osteogenic cells from Tg mice also had reduced mineralization ability *in vitro* as observed by alizarin staining, however addition of EPO did not affect the mineralization of wt or Tg osteogenic cells (Figure 5E).

Osteocytes in Tg mice with *Epor* deletion in osteoblasts

Since osteogenic cells from Tg mice showed reduced differentiation and mineralization *in vitro*, we enumerated the number of osteoblasts lining the trabecular bone in control and Tg mice treated with ten daily doses of EPO or saline (Figure 6A–C). We did not find any significant differences in osteoblast numbers in any of the mice groups in both males and females. Osteoblasts become embedded in the extracellular matrix and become osteocytes which are the most abundant cells in the bone(15). We did not find any significant changes in alive osteocytes in both male and female Tg mice compared to controls with or without EPO administration (Figure 6D, 6E, 6H). Male mice did not show any significant changes in the number of dying osteocytes; there was a trend for increased number of empty lacunae in male Tg mice but this effect was not significant (Figure 6F, 6G). The number of dying osteocytes were higher in the Tg female mice (Figure 6I), which aligns with the reduction in cortical bone volume observed in the female Tg mice (Figure 3I), and EPO administration in these mice reduced the number of dying osteocytes (Figure 6I). There was a trend for more empty lacunae in female Tg mice compared to control groups but the results were not significant (Figure 6J). Osteocytes are important in maintaining bone homeostasis and disruption of osteocytes are linked to bone fragility(15). Previous studies have shown that osteocytes can regulate both trabecular and cortical bone remodeling(16). Thus, the increased number of dying osteocytes in female Tg mice and trend for increased empty lacunae in male Tg mice might also be contributing to the reduced trabecular bone in the transgenic mice.

Epor deletion in osteoblasts does not affect osteoclasts

Analysis of TRAP stained sections of femurs did not show any significant differences in the number of osteoclasts in male and female control or Tg mice with or without EPO administration (Figure 7A–C). Osteoclast cultures from the bone marrow of control and

Tg mice did not show any significant difference in differentiation (Figure 7D, 7E). The osteoclast area was increased in the cultures of Tg mice osteoclasts with 10 U of EPO (Figure 7F) however there was no difference in the area of resorption which measures osteoclast activity (Figure 7G). We observed a trend for reduced osteoclast activity in both control and Tg mice with 5U of EPO suggesting that absence of Epor in osteoblasts does not affect EPO signaling in osteoclasts.

Discussion

Functional Epor is expressed by several non-erythroid cells suggesting a broad regulatory role for EPO besides erythropoiesis(1). Recent reports on the effect of EPO on bone in animal models have shown that EPO treatment promotes bone healing during fracture but reduces bone when administered in healthy animals. We previously showed that absence of EPO signaling in non-erythroid cells results in reduced trabecular bone in male and female mice(12). In elderly men in Sweden with normal renal function, high plasma EPO associated with higher incidence of fracture risk(17). Here we assessed the effect of endogenous EPO signaling specifically on bone forming osteoblasts using Tg mice with targeted deletion of *Epor* in osteoblasts. We observe that endogenous EPO is important for bone development in both male and female mice and defective bone formation in Tg mice that lack *Epor* in osteoblasts increases with age. At four weeks of age, Tg male mice exhibit decreased trabecular bone volume and fewer trabeculae without any change in cortical bone. Female Tg mice at four weeks of age show reduction only in cortical thickness. By 12 weeks of age with increasing skeletal maturity, the importance of endogenous EPO signaling in osteoblasts is readily apparent in both genders with significant reduction in trabecular bone volume, number and connectivity density. In Tg mice trabecular bone volume is reduced by 22.2% in males and 29.6% in females compared to their respective littermate controls. In the cortical bone, only female Tg mice exhibit reduction in cortical bone volume with cortical bone mineral density and cortical thickness unchanged. These data show a prominent role for EPO in the maintenance of trabecular bone compared to cortical bone. Thus, in skeletally mature mice, lack of endogenous EPO signaling reduces trabecular bone in both male and female mice, evident first in male mice at 4 weeks of age but with a greater reduction in trabecular bone in female mice by 12 weeks of age. In this study, generation of Tg mice was carried out using mice with *Cre* recombinase under the control of *Osteocalcin* (*Bglap*) promoter crossed with mice bearing floxed *Epor* alleles. The *Osteocalcin-Cre* mediated floxed recombination of *Epor* occurred specifically in osteoblasts and not in non-skeletal tissues such as spleen or white adipose tissue which express high levels of *Epor* (Supplemental figure 1C). Mature osteoblasts selectively express Osteocalcin and the Cre-recombinase under the regulation of *Osteocalcin* promoter is expressed starting at E17, after bone development is complete(18). Therefore, the phenotype we observed in the Tg mice is due to the specific deletion of *Epor* in mature osteoblasts. Endogenous EPO expression is observed in the hindlimbs of neonatal mice but not in the bones of adult mice(10). Our experiments were performed in mice older than 4 weeks of age and thus we conclude that in these mice the source of endogenous EPO regulating EPO-Epor signaling in osteoblasts is mainly derived from the kidneys.

Exogenous EPO administration in mouse models been reported to be associated with reduction in trabecular bone(12), including at both low dose(14) and high dose of EPO(4). Similarly, here we found elevated EPO reduced trabecular bone in both male (38.4% reduction in bone volume) and female (40.9% reduction in bone volume) wild type mice. However, Tg mice treated with EPO exhibited sexually dimorphic response in bone. In male Tg mice, EPO administration showed a trend for reduced trabecular bone (~20% reduction in bone volume) that was not significant or as prominent to the bone loss in wild type mice suggesting that the bone reduction observed with elevated EPO in male mice is not exclusively mediated by EPO response in osteoblasts. In contrast, female Tg mice did not exhibit any EPO induced reduction in trabecular bone, providing evidence that bone reduction in response to elevated EPO in females is either entirely mediated by Epo-Epor signaling in osteoblasts or that there is a protective mechanism against EPO induced bone loss specifically in female mice. Hormones like estrogen have osteoprotective role by regulating osteocyte function specifically in female mice. Abolition of estrogen signaling in osteocytes decreased trabecular bone only in female mice not in male mice(19). In our experiments with female wild type mice, EPO administration results in significant reduction of bone even with intact estrogen signaling. However, in female Tg mice; the absence of heightened exogenous EPO response in osteoblasts might be permitting estrogen signaling in bone maintenance. Previously, it was shown EPO treatment reduced body fat accumulation in male mice in contrast to female mice where the protective effect of estrogen against diet-induced obesity was greater than EPO regulation of body fat and there was no change in body fat with EPO administration(20). The significant bone loss with EPO treatment not observed in Tg mice, suggest that the bone reduction observed with elevated EPO in male and female mice requires EPO response in osteoblasts and underscores the importance of EPO-Epor signaling in osteoblasts in bone reduction due to elevated EPO.

Decreased trabecular bone is often associated with increased bone marrow adipocytes(21). Mice with Epor restricted to erythroid tissue exhibit marked increase in fat depots such as white adipose tissue and bone marrow adipocytes and reduced bone formation(2),(12). However, in the current study with Tg mice where the EPO-Epor signaling is specifically ablated in mature osteoblasts, we did not observe any significant changes in the number of bone marrow adipocytes with decreased trabecular bone. These data suggest that EPO signaling in mature osteoblasts and adipocytes may be mutually exclusive and that trabecular bone reduction is not always associated with increased marrow adiposity. Furthermore, while EPO treatment in wt mice reduces bone and the number of bone marrow adipocytes, Tg mice treated with EPO exhibit only the reduction in bone marrow adipocytes.

Addition of EPO to human osteoblast cultures induces phosphorylation of JAK2 and STAT3 proteins indicating active EPO-EPOR signaling in osteoblasts(22). In our studies, primary osteogenic cultures from Tg mice showed that osteoblasts lacking endogenous EPO signaling have less differentiation potential and the measurement of ALP activity which is an indicator of osteoblast activity showed consistently decreased ALP activity throughout the 21- day culture period. This is consistent with our observation that targeted deletion of *Epor* in osteoblasts reduces bone volume and the similar reduction in bone volume in mice lacking HIF1/HIF2 signaling in osteoblasts(10). EPO treatment of osteoblasts derived from differentiated bone marrow stromal cells showed that at low doses EPO inhibits

osteoblast differentiation and mineralization while increased doses of EPO stimulate these two processes along with regulating *Alpl* and *Runx2* transcript levels (23). Unlike the control osteogenic cells, the Tg osteogenic cells with deletion of *Epor* did not respond to addition of exogenous EPO in the culture medium. Besides the protein activity, we also observed significant reduction in *Alpl* mRNA levels in Tg osteogenic cultures. We assayed the expression of several key osteogenic genes and found only *Alpl* and *Runx2* transcripts to have significantly differential expression in Tg osteogenic cells. Tissue-nonspecific alkaline phosphatase encoded by the *Alpl* gene is an enzyme expressed early in the process of calcification with essential roles in bone mineralization(24). *Runx2* is a runt related transcription factor required for osteoblast differentiation and deficiency of Runx2 in committed osteoblasts is associated with disrupted postnatal bone formation by decreasing osteoblast function(25). Bone homeostasis is maintained by the coupling of osteoblast-osteoclast activity, and synthesis of cytokines Rankl and Osteoprotegrin by osteoblasts is essential for osteoclast differentiation(26). We did not observe any changes in osteoclast differentiation and resorption in cultures or in bone sections, suggesting that the absence of endogenous EPO signaling in osteoblasts does not affect osteoclast differentiation or activity.

In conclusion, deletion of *Epor* in mature osteoblasts resulted in significant trabecular bone reduction in both male and female mice. The loss of EPO signaling in osteoblasts decreases their differentiation potential with reduction in *Alpl* and *Runx2* expression levels but does not affect osteoclast differentiation or marrow adiposity. On the other hand, with ablation of EPO signaling in osteoblasts, EPO treatment stimulated erythropoiesis and red blood cell production, but no longer induced trabecular bone reduction observed in male and female wt mice. These findings demonstrate a previously unrecognized role for endogenous EPO as an essential regulator of osteoblasts and a direct role for EPO in regulating the bone microenvironment independent of its erythropoietic function.

Supplementary Material

Refer to Web version on PubMed Central for supplementary material.

Acknowledgements

This work was supported by the Intramural Research Program of the National Institute of Diabetes and Digestive and Kidney Diseases.

Non-standard abbreviations

TRAP	Tartrate-resistant acid phosphatase
Alpl	Gene encoding tissue-nonspecific Alkaline phosphatase
BMD	bone mineral density
BV	bone volume
BCIP/NBT	5-Bromo-4-chloro-3-indolyl phosphate/Nitro blue tetrazolium

Ct	cortical
EPO	Erythropoietin
Epor	Erythropoietin receptor
H & E	Hematoxylin-Eosin
M-CSF	Macrophage colony-stimulating factor
MTT	Thiazolyl Blue Tetrazolium Blue
RANKL	Receptor activator of nuclear factor kappa-B ligand
Tg	Transgenic
Tb	trabecular
WAT	White adipose tissue
Wt	Wild type

References

1. Zhang Y, Wang L, Dey S, Alnaeeli M, Suresh S, Rogers H, Teng R, and Noguchi CT (2014) Erythropoietin action in stress response, tissue maintenance and metabolism. Int J Mol Sci 15, 10296–10333 [PubMed: 24918289]
2. Teng R, Gavrilova O, Suzuki N, Chanturiya T, Schimel D, Hugendubler L, Mammen S, Yver DR, Cushman SW, Mueller E, Yamamoto M, Hsu LL, and Noguchi CT (2011) Disrupted erythropoietin signalling promotes obesity and alters hypothalamus proopiomelanocortin production. Nat Commun 2, 520 [PubMed: 22044999]
3. Beleslin-Cokic BB, Cokic VP, Yu X, Weksler BB, Schechter AN, and Noguchi CT (2004) Erythropoietin and hypoxia stimulate erythropoietin receptor and nitric oxide production by endothelial cells. Blood 104, 2073–2080 [PubMed: 15205261]
4. Hiram-Bab S, Liron T, Deshet-Unger N, Mittelman M, Gassmann M, Rauner M, Franke K, Wielockx B, Neumann D, and Gabet Y (2015) Erythropoietin directly stimulates osteoclast precursors and induces bone loss. FASEB J 29, 1890–1900 [PubMed: 25630969]
5. Ott C, Martens H, Hassouna I, Oliveira B, Erck C, Zafeiriou MP, Peteri UK, Hesse D, Gerhart S, Altas B, Kolbow T, Stadler H, Kawabe H, Zimmermann WH, Nave KA, Schulz-Schaeffer W, Jahn O, and Ehrenreich H (2015) Widespread Expression of Erythropoietin Receptor in Brain and Its Induction by Injury. Mol Med 21, 803–815 [PubMed: 26349059]
6. Ogilvie M, Yu X, Nicolas-Metral V, Pulido SM, Liu C, Ruegg UT, and Noguchi CT (2000) Erythropoietin stimulates proliferation and interferes with differentiation of myoblasts. J Biol Chem 275, 39754–39761 [PubMed: 10995753]
7. Zaidi M (2007) Skeletal remodeling in health and disease. Nat Med 13, 791–801 [PubMed: 17618270]
8. Garcia P, Speidel V, Scheuer C, Laschke MW, Holstein JH, Histing T, Pohlemann T, and Menger MD (2011) Low dose erythropoietin stimulates bone healing in mice. J Orthop Res 29, 165–172 [PubMed: 20740668]
9. Wan L, Zhang F, He Q, Tsang WP, Lu L, Li Q, Wu Z, Qiu G, Zhou G, and Wan C (2014) EPO promotes bone repair through enhanced cartilaginous callus formation and angiogenesis. PLoS One 9, e102010 [PubMed: 25003898]
10. Rankin EB, Wu C, Khatri R, Wilson TL, Andersen R, Araldi E, Rankin AL, Yuan J, Kuo CJ, Schipani E, and Giaccia AJ (2012) The HIF signaling pathway in osteoblasts directly modulates erythropoiesis through the production of EPO. Cell 149, 63–74 [PubMed: 22464323]

11. Wang L, Teng R, Di L, Rogers H, Wu H, Kopp JB, and Noguchi CT (2013) PPARalpha and Sirt1 mediate erythropoietin action in increasing metabolic activity and browning of white adipocytes to protect against obesity and metabolic disorders. Diabetes 62, 4122–4131 [PubMed: 23990359]
12. Suresh S, de Castro LF, Dey S, Robey PG, and Noguchi CT (2019) Erythropoietin modulates bone marrow stromal cell differentiation. Bone Research 7, 21 [PubMed: 31666996]
13. McKenzie J, Smith C, Karuppaiah K, Langberg J, Silva MJ, and Ornitz DM (2019) Osteocyte Death and Bone Overgrowth in Mice Lacking Fibroblast Growth Factor Receptors 1 and 2 in Mature Osteoblasts and Osteocytes. J Bone Miner Res 34, 1660–1675 [PubMed: 31206783]
14. Singbrant S, Russell MR, Jovic T, Liddicoat B, Izon DJ, Purton LE, Sims NA, Martin TJ, Sankaran VG, and Walkley CR (2011) Erythropoietin couples erythropoiesis, B-lymphopoiesis, and bone homeostasis within the bone marrow microenvironment. Blood 117, 5631–5642 [PubMed: 21421837]
15. Delgado-Calle J, and Bellido T (2015) Osteocytes and Skeletal Pathophysiology. Curr Mol Biol Rep 1, 157–167 [PubMed: 26693137]
16. Canalis E, Adams DJ, Boskey A, Parker K, Kranz L, and Zanotti S (2013) Notch signaling in osteocytes differentially regulates cancellous and cortical bone remodeling. J Biol Chem 288, 25614–25625 [PubMed: 23884415]
17. Kristjansdottir HL, Lewerin C, Lerner UH, Herlitz H, Johansson P, Johansson H, Karlsson M, Lorentzon M, Ohlsson C, Ljunggren O, and Mellstrom D (2020) High Plasma Erythropoietin Predicts Incident Fractures in Elderly Men with Normal Renal Function: The MrOS Sweden Cohort. J Bone Miner Res 35, 298–305 [PubMed: 31626711]
18. Elefteriou F, and Yang X (2011) Genetic mouse models for bone studies--strengths and limitations. Bone 49, 1242–1254 [PubMed: 21907838]
19. Kondoh S, Inoue K, Igarashi K, Sugizaki H, Shirode-Fukuda Y, Inoue E, Yu T, Takeuchi JK, Kanno J, Bonewald LF, and Imai Y (2014) Estrogen receptor alpha in osteocytes regulates trabecular bone formation in female mice. Bone 60, 68–77 [PubMed: 24333171]
20. Zhang Y, Rogers HM, Zhang X, and Noguchi CT (2017) Sex difference in mouse metabolic response to erythropoietin. FASEB J 31, 2661–2673 [PubMed: 28283542]
21. Shu L, Beier E, Sheu T, Zhang H, Zuscik MJ, Puzas EJ, Boyce BF, Mooney RA, and Xing L (2015) High-fat diet causes bone loss in young mice by promoting osteoclastogenesis through alteration of the bone marrow environment. Calcif Tissue Int 96, 313–323 [PubMed: 25673503]
22. Guo L, Luo T, Fang Y, Yang L, Wang L, Liu J, and Shi B (2014) Effects of erythropoietin on osteoblast proliferation and function. Clin Exp Med 14, 69–76 [PubMed: 23135151]
23. Rauner M, Franke K, Murray M, Singh RP, Hiram-Bab S, Platzbecker U, Gassmann M, Socolovsky M, Neumann D, Gabet Y, Chavakis T, Hofbauer LC, and Wielockx B (2016) Increased EPO Levels Are Associated With Bone Loss in Mice Lacking PHD2 in EPO-Producing Cells. J Bone Miner Res 31, 1877–1887 [PubMed: 27082941]
24. Orimo H (2010) The mechanism of mineralization and the role of alkaline phosphatase in health and disease. J Nippon Med Sch 77, 4–12 [PubMed: 20154452]
25. Adhami MD, Rashid H, Chen H, Clarke JC, Yang Y, and Javed A (2015) Loss of Runx2 in committed osteoblasts impairs postnatal skeletogenesis. J Bone Miner Res 30, 71–82 [PubMed: 25079226]
26. Boyce BF, and Xing L (2007) Biology of RANK, RANKL, and osteoprotegerin. Arthritis Res Ther 9 Suppl 1, S1 [PubMed: 17634140]

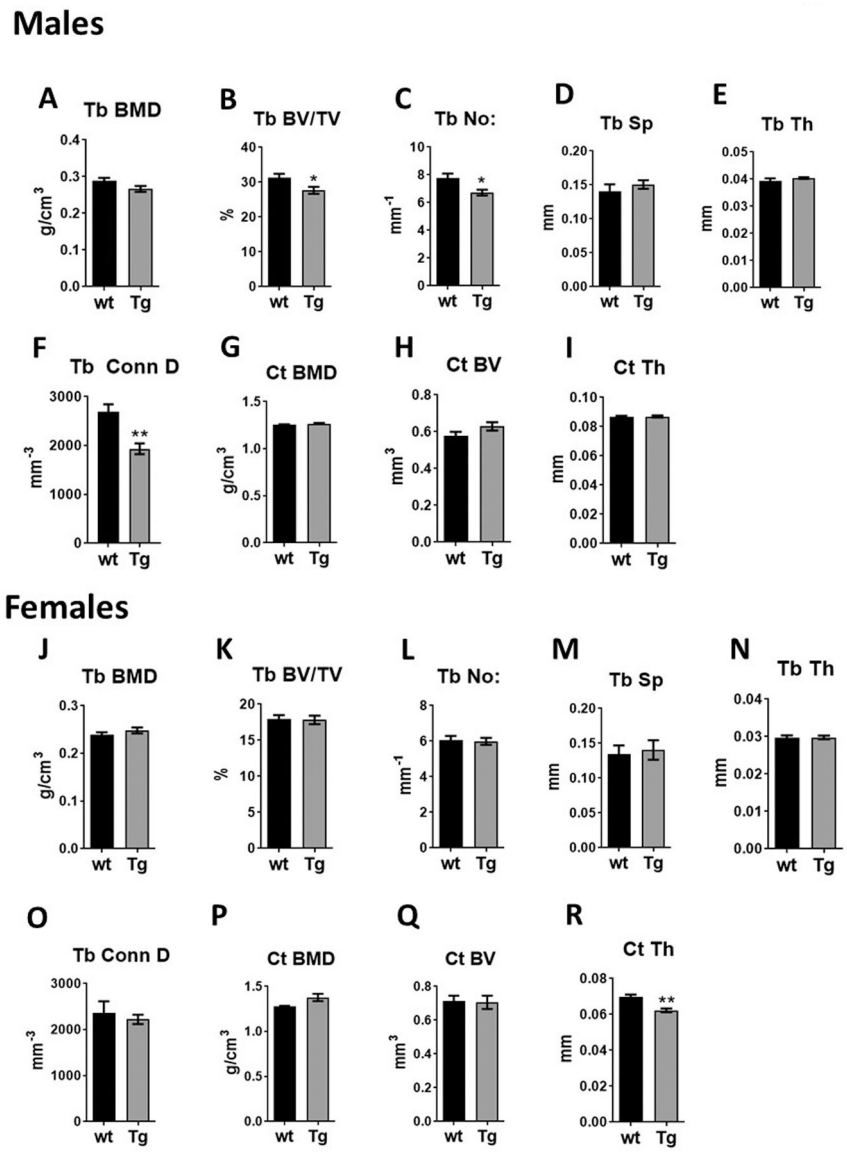

Figure 1:

Bone features of 4-week-old male and female transgenic mice (Tg) with Epor deletion in osteoblasts and littermate controls (wt). **(A-F)** Micro-CT quantification of trabecular parameters in male mice including trabecular (Tb) bone mineral density (BMD), bone volume/tissue volume (BV/TV), number (No:), spacing (Sp), Thickness (Th) and connectivity density (Conn D). **(G-I)** Micro-CT quantification of cortical BMD, BV and thickness in male mice. **(J-O)** Micro-Ct quantification of trabecular parameters in female mice. **(P-R)** Quantification of cortical bone parameters in female mice. (n=5/group, *p<0.05, **p<0.01).

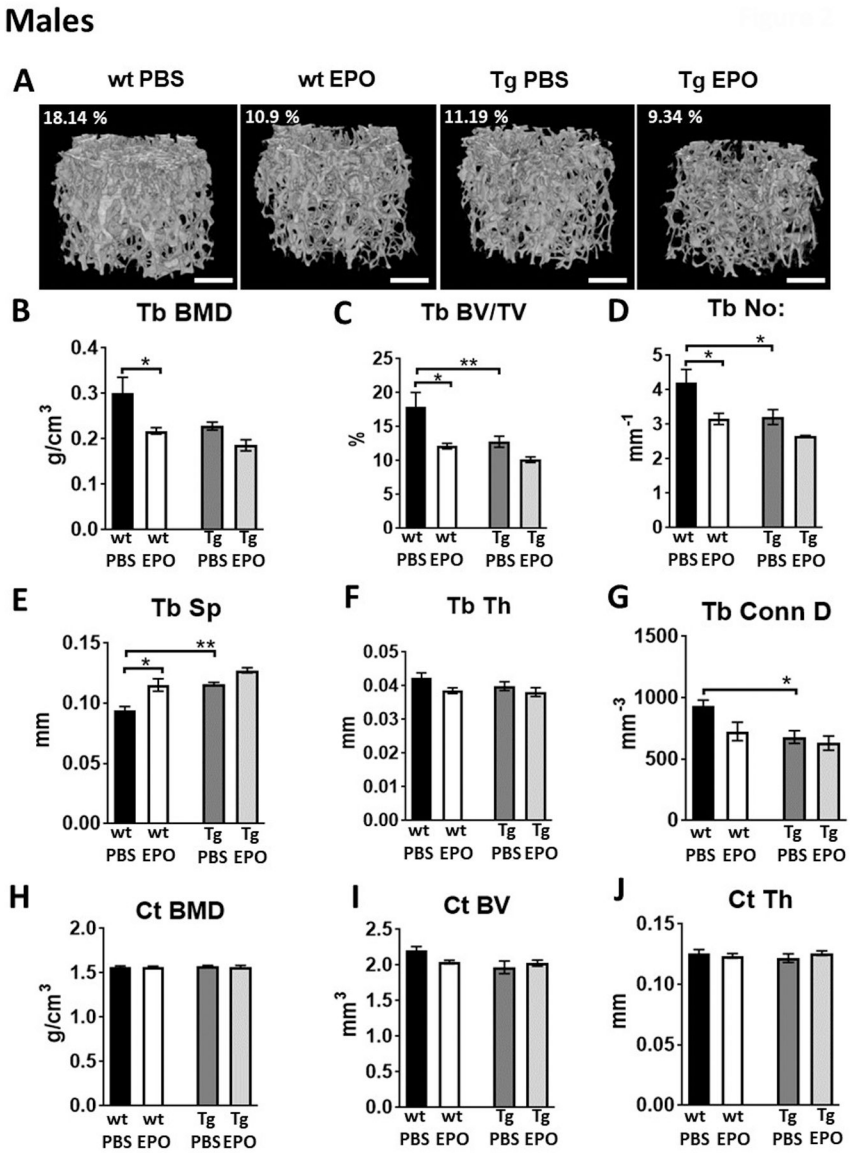

Figure 2:

Bone features of 12-week-old male transgenic mice (Tg) with Epor deletion in osteoblasts and littermate controls (wt) with 10 daily administration of recombinant Epo. **(A)** 3D images of trabecular bones of wt and Tg male mice receiving 1200 IU/kg of EPO for ten days. **(B-G)** Micro-CT quantitation of trabecular BMD, trabecular BV/TV, number, spacing, thickness and connectivity density. **(H-J)** Micro-CT quantitation of cortical BMD, BV and thickness. (n=4–6/group, *p<0.05, **p<0.01).

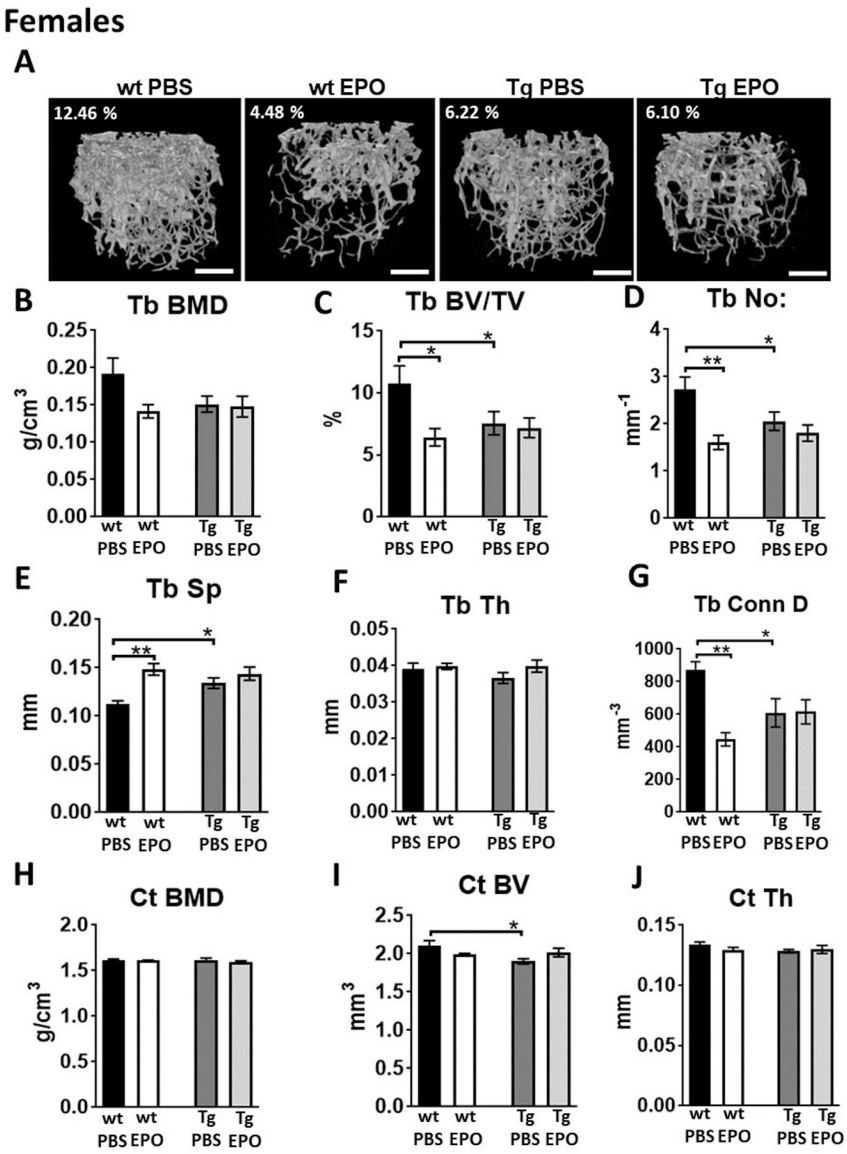

Figure 3:

Bone features of 12-week-old female transgenic mice (Tg) with Epor deletion in osteoblasts and littermate controls (wt) with 10 daily administration of recombinant EPO. **(A)** 3D images of trabecular bones of wt and Tg female mice receiving 1200 IU/kg of EPO for ten days. **(B-G)** Micro-CT quantitation of trabecular BMD, trabecular BV/TV, number, spacing, thickness and connectivity density. **(H-J)** Micro-CT quantitation of cortical BMD, BV and thickness. (n=4–6/group, *p<0.05, **p<0.01).

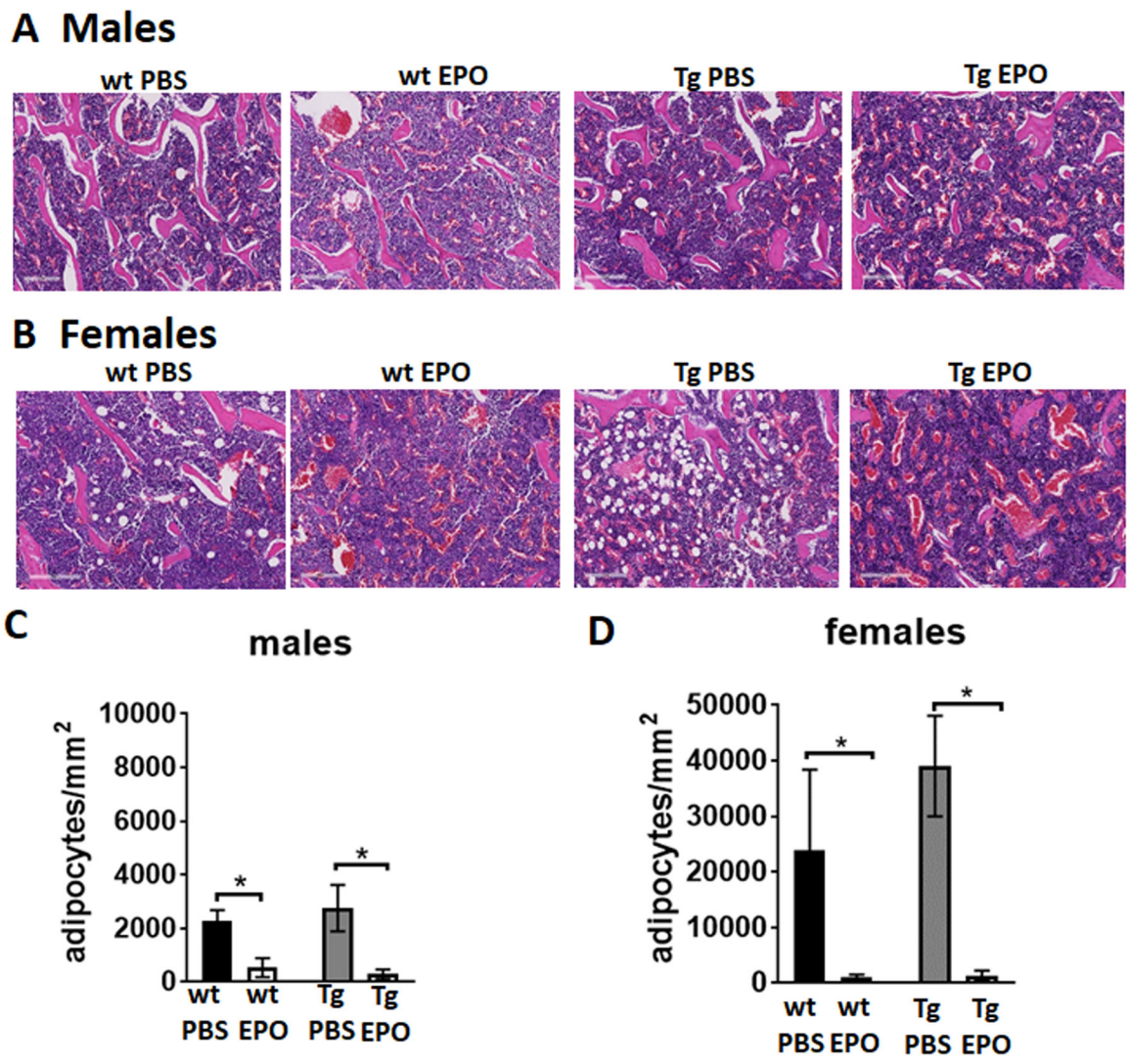

Figure 4:

Histology analysis by H & E staining of femur sections of 12-week-old male and female wt and Tg mice receiving 1200 IU/kg of EPO for ten days. **(A-B)** Femurs of 12-week-old male **(A)** and female **(B)** Tg mice and controls. Bone marrow adipocytes appear as white circles in the marrow, pink colored regions are bones and blue regions are the bone marrow (n=4–6/group), scale bar 200 μm **(C-D)** Number of bone marrow adipocytes in femurs of male **(C)** and female **(D)** Tg mice per mm^2 of the marrow (n=4–6/group). *p<0.05, **p<0.01).

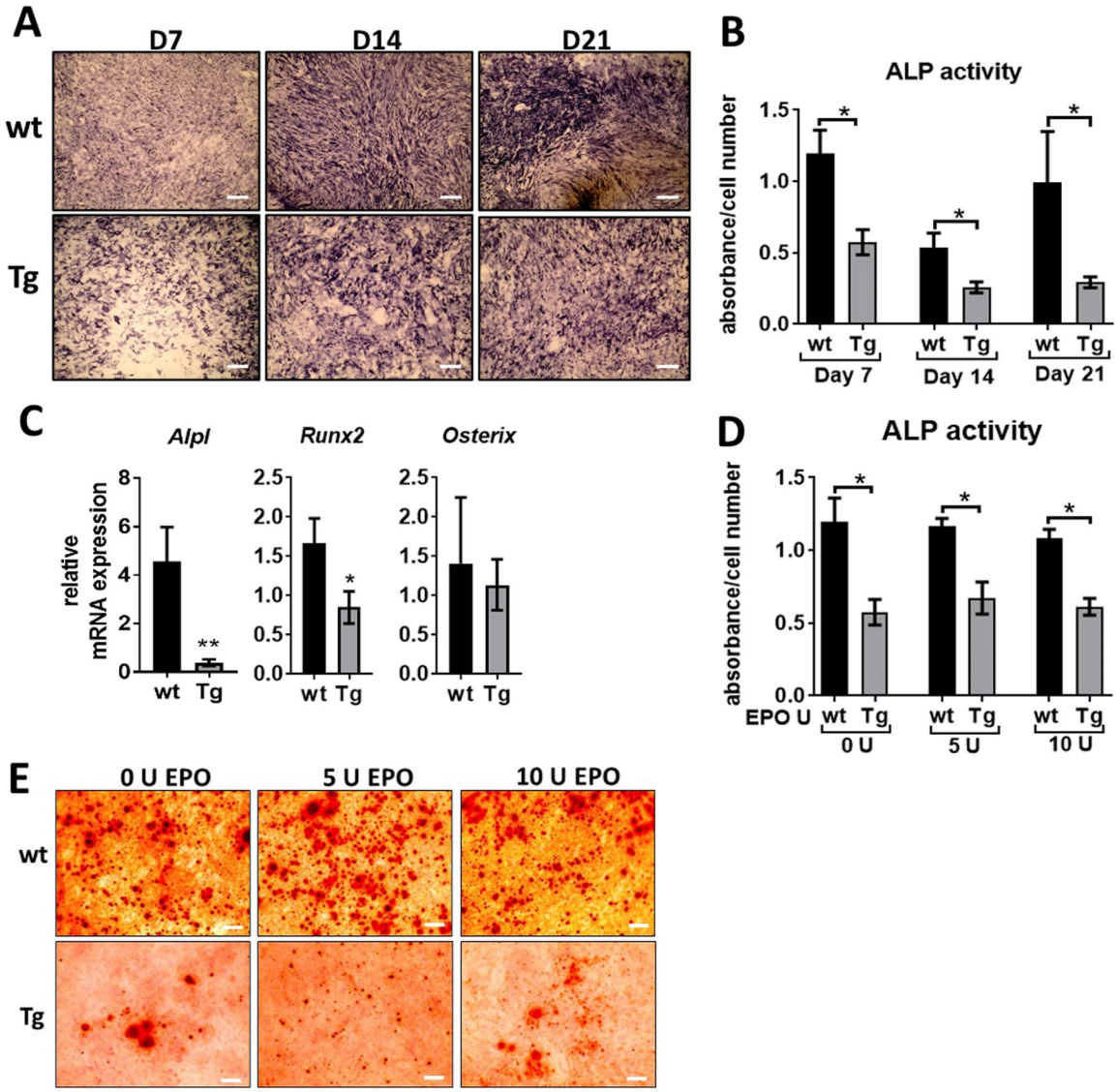

Figure 5:

Osteogenic cultures of Tg mice and littermate controls. **(A)** Calvarial osteoprogenitors isolated from wt and Tg mice were cultured in osteogenic medium and stained for ALP expression on day 7, 14 and 21, scale bar 50 μm. **(B)** ALP activity was measured using a colorimetric assay and expressed as absorbance normalized to the cell number determined by MTT assay. **(C)** Relative mRNA expression of *Alpl*, *Runx2* and *Osterix* in osteogenic cultures on day 7 determined by real-time PCR, fold changes expressed relative to the expression in wt osteogenic cells. **(D)** Calvarial osteogenic cells from wt and Tg mice treated with 5 U and 10 U of EPO for 24 hours and ALP activity measured using colorimetric assay, absorbance was normalized to the cell number. **(E)** Calvarial osteoprogenitors from wt and Tg mice stained for mineralization using alizarin staining after 28 days of culture in osteogenic medium, scale bar 50 μm. (n=4/group, *p<0.05, **p<0.01).

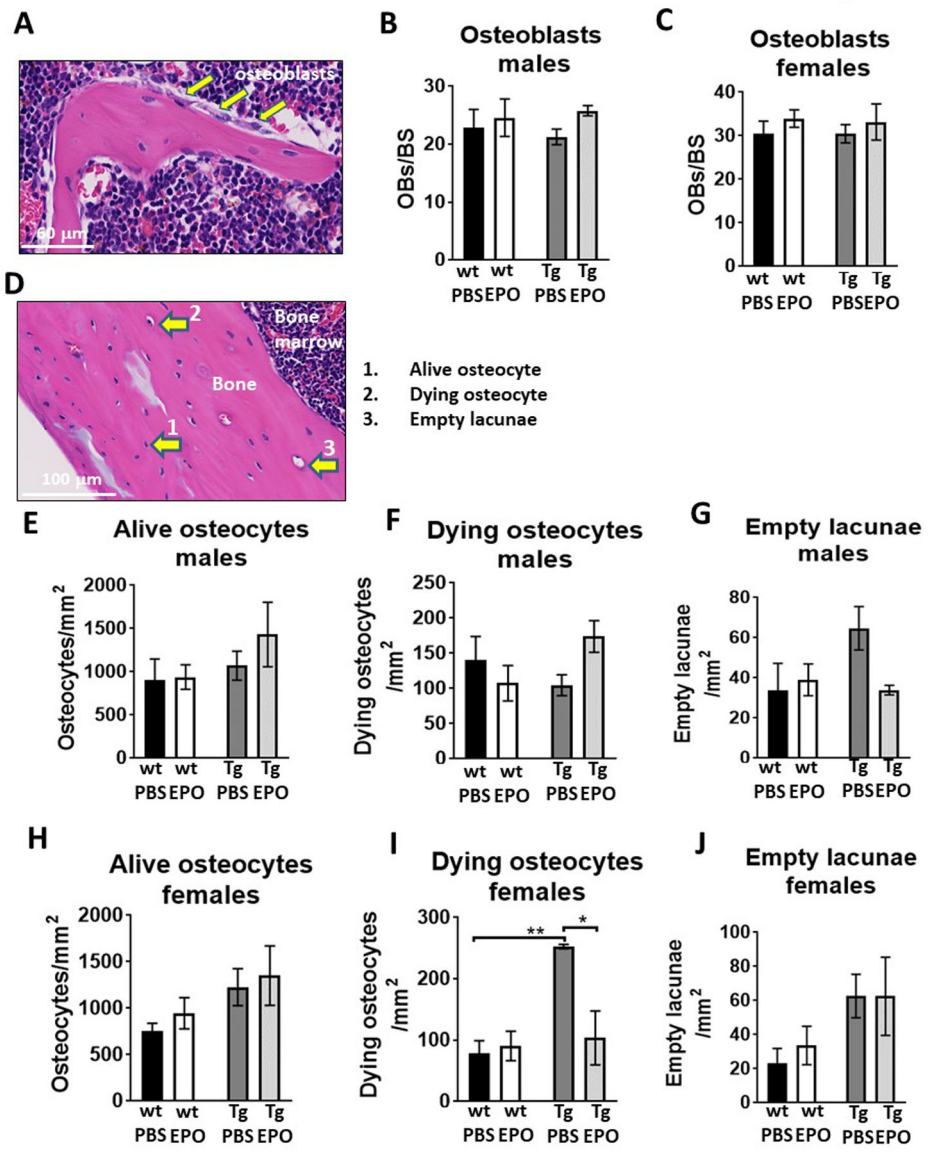

Figure 6.

Osteoblast and osteocyte quantification. **(A)** H & E stained section of trabecular bone with osteoblasts on the surface. **(B-C)** Enumeration of number of osteoblasts per bone surface in male **(B)** and female **(C)** wt and Tg mice with either saline or EPO treatment. **(D)** H & E stained section of cortical bone showing alive osteocytes, dying osteocyte and empty lacunae. **(E-J)** Quantification of osteocytes (alive, dying) and empty lacunae in males **(E-G)** and female **(H-J)** mice per mm^2.

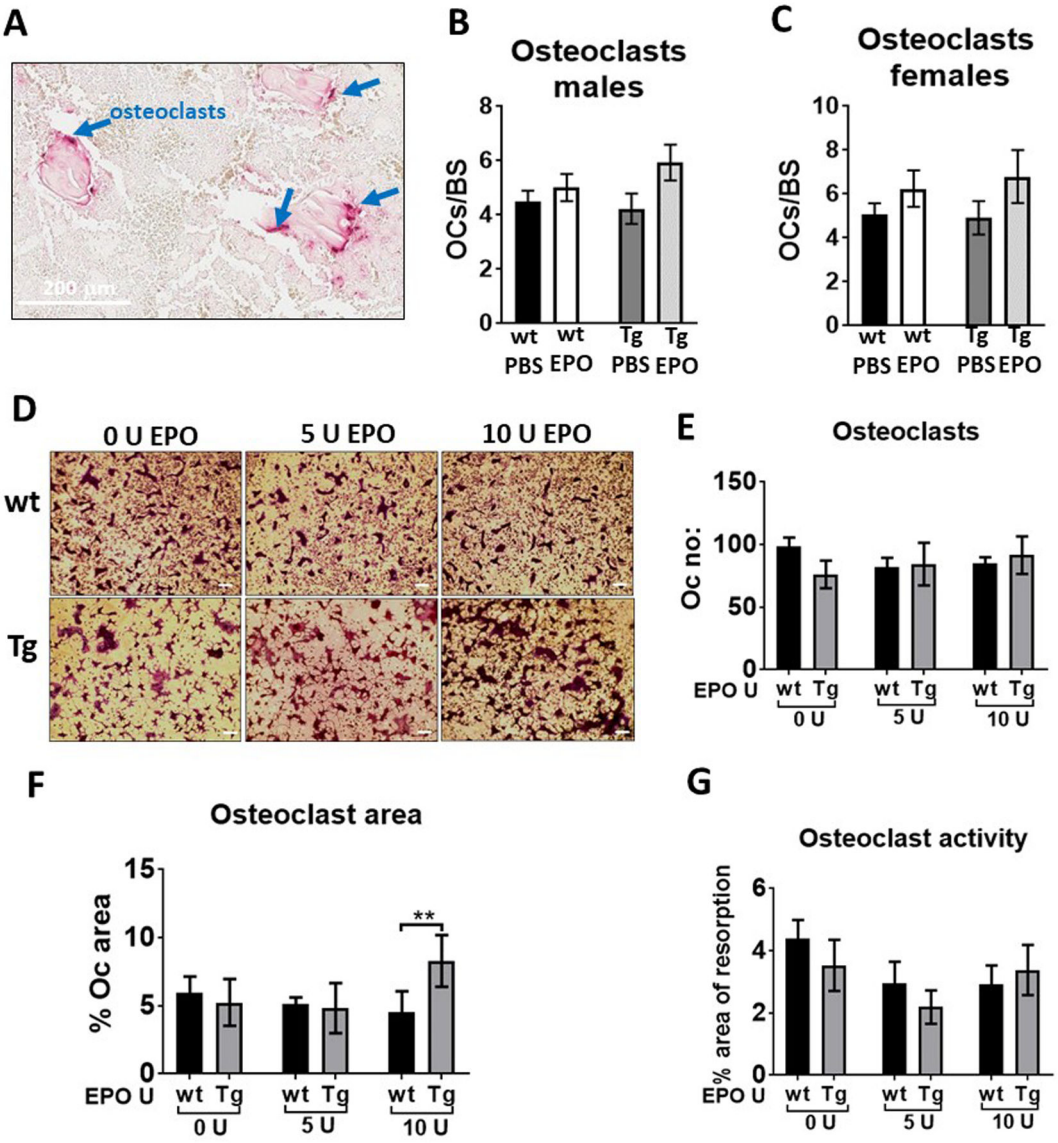

Figure 7:

Enumeration of osteoclasts *in vivo* and *in vitro* in Tg mice and littermate controls. **(A)** Image of TRAP positive osteoclasts on the surface of trabecular bone. **(B-C)** quantification of TRAP positive osteoclasts per bone surface in male **(B)** and female **(C)** wt and Tg mice with either saline or EPO treatment. **(D)** Images of *in vitro* osteoclast differentiation of bone marrow cells of wild type (wt) and Tg mice using M-CSF and RANKL. Osteoclasts appear after 4–5 days and were stained for TRAP, scale bar 50 μm. **(E)** Enumeration of number of TRAP stained osteoclasts in culture using ImageJ analysis software. **(F)** Quantitation of osteoclast area in cultures using ImageJ analysis software. **(G)** Quantitation of osteoclast activity by counting area of resorption using Corning Osteo assay surface plates (n=5/group).

Table 1

Primers and probes used for real-time PCR

Primers and probes		**Sequences**
Alkaline phosphatase	FP	TTGTGCCAGAGAAAGAGAGAGA
	RP	GTTTCAGGGCATTTTTCAAGGT
Runx2	FP	ACGAAAAATTAACGCCAGTCG
	RP	TCGGTCTGACGACGCTAAAG
Osterix	FP	GAGGAAGAAGCTCACTATGGCTCCAG
	RP	GCCTCCTTTCCCCAGGGTTGTTGA
β-actin	FP	GCAGGAGTACGATGAGTCCG
	RP	ACGCAGCTCAGTAACAGTCC
Rankl	FP	TTTCGAGCGCAGATGGATCC
	RP	CCTGCAAATCTGCGTTTTCATGGA
Col1a1	FP	ACTGCCCTCCTGACGCATGGCCAAG
	RP	CGTGCCATTGTGGCAGATACAGAT
Osteoprotegrin	FP	AGTGAGGAGGAAGACATTGTGTGT
	RP	GGGCTGCAATACACACACTCATC
Epor	FP	GCTCCGGGATGGACTTCA
	RP	GAGCCTGGTGCAGGCTACAT
	Probe	CATACCAGCTCGAGGGTGAGTCACGAAAG
S16	FP	GATCGAGCCGCGCACG
	RP	CAAATCGCTCCTTGCCCA
	Probe	CTGCAGTACAAGTTACTGGAGCCTGTTTTGCT